Journal of Chromatography A 1751 (2025) 465951

Contents lists available at ScienceDirect

Journal of Chromatography A

journal homepage: www.elsevier.com/locate/chroma

Extended multidimensional design space studies: Comparing volatile and non-volatile buffer systems in UPLC

Arnold Zöldhegyi [a,b], Barnabás Soós [a,c], Krisztián Horváth [a], Imre Molnár [b], Róbert Kormány [c,*]

[a] Department of Analytical Chemistry, University of Pannonia, Egyetem u. 10, 8200 Veszprém, Hungary
[b] Molnár-Institute for Applied Chromatography, Schneeglöckchenstrasse 47, 10407 Berlin, Germany
[c] Egis Pharmaceuticals Plc., Keresztúri út 30-38, Budapest, Hungary

ARTICLE INFO

Keywords:
pH-selection in reversed phase chromatography
Volatile
Non-volatile buffer interchangeability
Salting-out Effects
Analytical quality by design
Design space comparison

ABSTRACT

Selecting the appropriate pH modifiers for separating ionizable compounds in HPLC often presents complex challenges that are frequently overlooked by industry practitioners. In Reversed-Phase Chromatography (RPC), defining pH is particularly problematic due to the presence of organic solvents, which influence the dissociation behavior of buffering agents, ionizable analytes, and residual silanol groups on the silica base material. Additional factors such as temperature changes and varying buffering capacities further complicate the interpretation of pH-effects on the separation.

A key practical question arises: can a volatile acetate buffer effectively replace an equimolar non-volatile phosphate buffer within the same pH range? To explore this, we utilized an Analytical Quality by Design (AQbD) modeling approach with DryLab to construct and compare three-dimensional (t_G-T-pH) separation models for terazosin and selected impurities across a pH range of 6.0–8.0. These Design Space (DS) models provided a comprehensive understanding of the dynamic changes occurring within each separation system. Notably, our findings revealed not only equivalent separation performance, as indicated by overlapping Method Operable Design Regions (MODRs), but also critical insights into buffer-specific differences in the selectivity of HPLC-separations.

1. Introduction

In high-pressure liquid chromatography (HPLC), numerous parameters influence chromatographic selectivity. While the wide range of available selectivity options offers nearly limitless possibilities for achieving desired separation goals, this can also impose a significant challenge for the developer.

Understanding the role of relevant parameters and exploring their individual and combined effects on the retention properties of analytes has always been a central focus in liquid chromatography to optimize the separation process. Chromatographic parameters of a separation system can generally be divided into two main groups: "hard-to-change" or "qualitative" variables, such as the selected stationary phase and the specific instrument used for analysis, and continuous parameters, including mobile phase composition (%B), flow rate (F), and column temperature (T). The latter group is ideal for selectivity tuning, as these parameters can be easily adjusted without major modifications to the chromatographic setup [1,2].

In Reversed-Phase Chromatography (RPC), further selectivity can be explored by mixing various strong solvents (“ternary” composition”) or by adjusting the pH, especially in the presence of ionogenic substances. The significance of these factors has been thoroughly investigated since the early days of HPLC. For example, by treating the sorption-desorption processes as thermodynamic phenomena, Csaba Horváth’s solvophobic interaction theory identified all relevant parameters influencing the capacity factors. These included %B (or $\%H_2O$, which exhibits lipophobic properties), T, pH, stationary phase properties, and in ion-pairing (IP-RP) applications, the buffer-, and ion-pairing reagent ("Hetaeron"), and salt concentration [3–5].

However, contrary to the other parameters, pH has a conditional value, representing only the relative acidity of a solution. Indeed, pH is an operational parameter, not directly linked to the absolute concentration of hydronium cations ($[H_3O^+]$), but rather to the actual hydronium cation activity (α_{H3O+}). Hence, the effective concentration is

* Corresponding author.
E-mail address: kormany.robert@egis.hu (R. Kormány).

https://doi.org/10.1016/j.chroma.2025.465951
Received 27 February 2025; Received in revised form 7 April 2025; Accepted 9 April 2025
Available online 10 April 2025
0021-9673/© 2025 Elsevier B.V. All rights are reserved, including those for text and data mining, AI training, and similar technologies.

usually described by an activity coefficient (γ), which accounts for additional dependencies—that is the standard state of hydronium cation activity in the solvent and the temperature (T). This further, less evident dependence already leads to significant confusions among HPLC practitioners, when solvents with water in mixture are used (e.g., water-organic mixtures). In such cases, pH can be defined on two relative scales: One specific to the solvent and the other to water. However, chromatographic techniques like RPC and hydrophilic interaction chromatography (HILIC) often use organic-rich eluents as the mobile phase. In contrast, in everyday use pH is simply defined in pure aqueous solutions. In an analytical laboratory, pH is measured in full-aqueous solution usually with a hydrogen-ion selective glass electrode filled with a standard buffer (e.g., 3 M KCl). Such a well-calibrated pH meter produces objective and reliable results—as long as the sample solvent is dilute, aqueous, and has a midrange pH. In comparison, determining the exhibited acidic nature of a given sample solution with this conventional setup becomes more challenging when various mixtures of organic eluents are added. Significant differences arise in consequence of several physicochemical factors. First, the junction potential term of a standard glass electrode becomes substantial due to prevailing charge separation between the aqueous filling solution and the organic sample solution. Second, the standard 0–14 pH range expands, due to different autoprotolysis constants in organic eluents, such as methanol or acetonitrile ($K_{MeOH} = 10^{-16.6}$, $K_{ACN} = 10^{-33.58}$ at 25 °C). Finally, the dissociation rates of acids and bases can significantly vary in presence of organic solvents, compared to their, in water defined pK_a-values [6–8].

Naturally, when it comes to the selection of pH-additives, it is often established either with a simple alkaline or acidic modifier. From the practical standpoint, this is a reasonable choice, because at two ends of the pH-range the hydronium-, and hydroxyl-ions ensure tremendous buffering capacity. However, accurate pH specification becomes harder, when considering intermediate pH-range, prepared with a buffer system, comprised of solutions of a weak acid and its conjugate base, or a weak base and its conjugate acid. Here pH and the stabilizing effect of the buffer capacity can change by various degrees. Today, there are numerous buffers used for LC operations, some are non-volatile, while others are readily volatile, making them particularly useful for mass spectrometry applications. However, as it will be discussed in this paper, under RP-conditions, it is not only extremely important to initially select an appropriate pH-modifier or a buffer system but also take into account possible pH-shifts, accompanied by drastically altered chromatographic selectivities [6,9–11].

Although it is theoretically possible to scale and convert between aqueous pH and their respective pH equivalents in certain organic-aqueous solvents using thermodynamic acid-base constants, this method can be less accurate and therefore less workable in practice. This is especially true in gradient elution, where the rapid change in aqueous-organic composition within the separation system impedes any practical conversion [6]. Additionally, research by Rosés demonstrated that pH variations are not only influenced by the choice of the given organic solvent and temperature but also by the actual buffering solution used [8]. This can lead to some unexpected pH developments, as also reported by Claassens and colleagues [12]. In their work, they mixed equal amounts of pH = 10 aqueous phosphate and glycine buffers with methanol and were surprised to find that their silica-based stationary phase dissolved ~10 times faster in the phosphate-buffered mobile phase, than in the glycine-buffered one. Follow-up investigation by Tindall and Perry found that the addition of methanol shifted the pH insignificantly for the glycine buffer but as high as 10.8 for the phosphate buffer, which ultimately led to the accelerated dissolution of the silica base material [13]. Clearly, when an organic solvent is added to an aqueous buffer, both dilution effects and pK_a-shifts of the buffering species occur almost simultaneously. Generally, the pK_a-values of neutral acids (like formic acid) and anionic acids (like $H_2PO_4^-$) tend to shift to higher values, whereas cationic acids (like NH_4^+) behave in the opposite manner [8,14]. However, as Tindall again pointed out, reversed trends and more complex responses are also possible [7]. In addition, when considering methanol and acetonitrile, they have significantly lower dielectric constants and are weaker bases than water, resulting again in different abilities to dissociate ions [6].

Given all these complexities, it is much simpler and more reproducible to prepare the aqueous buffer before mixing it with the organic modifier. Here, other than performing the pH measurements with the conventional laboratory pH-meter, one can also use the “weights-and-volumes” method for more precise and reproducible pH measurement. Nevertheless, either method is used, it’s always crucial to step-by-step document eluent preparations and the ways of actual pH measurements in every detail to ensure maximum pH-reproducibility [15,16]. Another key practical consideration is the solubility of various buffer salts. Solubility is influenced by the type of buffer, its concentration, and the nature and proportion of the organic modifier in the mobile-phase. Generally, hydro-organic solutions with salt concentrations below 10 mM are unlikely to precipitate the salt under most of the applied %B conditions. However, solubility issues are well-known, when working with acetonitrile and sodium or ammonium phosphate buffer solutions at concentrations of approximately 25–50 mM under neutral pH conditions [6,17].

Finally, the acidic residual silanol groups on silica-based packings can further pose some more influence on the already tangled pH relationships. This is particularly true when operating near their respective pK_a values, where some of the heterogenous, various types of residual silanol groups start to dissociate. Newer, synthetic "Type B" high-purity silica columns have lower metal impurities, which results in silanol groups with a less acidic character ($pK_a \approx 6$). Consequently, compared to older "Type A" silica, modern "Type B" columns, especially when packed in narrow-bore formats, require significantly lower buffer concentrations (~5–10 mM) to maintain energetic homogeneity, particularly concerning the residual silanol groups [6,7,10,18,19].

In conclusion, it is important to note that in RPC there are multifold interactions formed between mobile phase, solute molecules and the stationary phase. Therefore, certain pH developments cannot be reliably assessed without proper systematic experimental support. Traditional method development routines provide only limited guidance in this area. To fully harness the potential of pH settings—an immensely powerful tool for manipulating peak positions to achieve optimal chromatographic selectivities—more comprehensive experimental strategies are essential. Specifically, employing Design of Experiments (DoE) approaches can provide the structured framework needed for effective exploration and optimization.

These thoughts are in alignment with most recent regulatory guidelines on Analytical Quality by Design (AQbD) that endorse industry using systematic working methodologies for better understanding of factor-response relationships. The main advantage of following such a structured approach is the acquisition of multidimensional Design Space (DS) with profound understanding of the relationships between relevant analytical variables and measured responses. Within this space, Method Operable Design Region (MODR) can be outlined, which is a smaller subset of parameter ranges where the analytical procedure performance criteria (Analytical Target Profile) are continuously fulfilled and the quality of the measured result is assured. In other words, when working within the multidimensional MODR, *changes to the workpoint do not require additional regulatory notification*. Thus, following such AQbD approaches, post-approval changes can easily be managed at lesser need of regulatory oversight, if the changes are documented properly using modeling. AQbD builds trust and leads to a more effective communication between the applicant and regulatory bodies [20–22].

The development of methods using computerized tools to build in-silico knowledge of complex chromatographic systems was pioneered by Laub and Purnell in the 1970s. They introduced "window diagrams" to visualize the effects of relevant parameters in both GC and LC and introduced the term of the “critical resolution”, identifying how varying conditions (e.g., temperature or pH) can cause peaks to cross [23]. This

very early spurred further investigation into method optimization using these diagrams. In 1978, Deming optimized RPC by studying the effect of pH on the selectivity of weak organic acids, emphasizing the importance of finding both local and global optima to achieve separation goals in the shortest analysis time [24]. Price later demonstrated the practical advantages of "window plots" in separating complex samples, such as cinnamic acids and related compounds [25]. By 1980, Sachok et al., described a two-factor systematic approach, exploring the interaction between pH and ion-pair reagent concentration to predict the separation of a nine-compound sample. Their response surfaces made it easy to identify optimal conditions and assess method robustness [26].

The pH modeling capability was significantly improved by the LC-Resources team in their commercial software suite, DryLab I/mp (= isocratic/multiparameter version). Their goal was to provide accurate predictions of mobile phase parameter effects on HPLC separations across a broad range of conditions, with a minimal number of initial experimental runs (typically 2 or 3 per factor). They recognized that the retention factor (*k*) can change dramatically between ionized and non-ionized compounds, often requiring a combination of pH optimization and solvent strength (%B) variation to maintain a reasonable *k*-range (1–20) for effective separations. In the first version of their software, they developed a “restricted” multi-parameter mapping scheme to investigate and optimize method parameters under isocratic elution conditions [27–30]. Later, they established the groundwork for true multidimensional modeling by incorporating gradient conditions (steepness, range, and shape) alongside temperature—for two of the most critical factors influencing selectivity. They employed a simple, straightforward 2 × 2 Design of Experiments (DoE) approach to quantify the selectivity-changing effects of both parameters for neutral (regular) and ionizable (irregular) compounds [31–34]. The software’s visualization capabilities soon evolved, allowing for the creation of monochromatic 2-dimensional “heat maps” (“Critical Resolution Maps”), that illustrated interactions between variables, such as multidimensional variations of %B or gradient time (t_G), temperature (T), pH, and other selected factors such as column length, column diameter, particle size, flow rate, positions of gradient points (time and %B-values), dwell volume and extra-column volume [35–37].

A significant milestone in chromatographic method development was the simultaneous coupling of three key experimental variables—gradient time, temperature and either pH or ternary composition—within a single virtual model. This three-dimensional space, termed “Design Space (DS)” or simply the "Cube," allowed for continuous investigation of critical resolution changes for a sample on a particular stationary phase, depending on relevant mobile phase parameters. This comprehensive approach streamlined the identification of workable MODR, enabling the establishment of robust HPLC regions with greater flexibility for routine applications in case of deviations from the expected and validated behavior of separations in industrial Quality Control (QC) environment [38,39].

Building on the same 12-input experimental model, Kormány and Molnár later applied simultaneous optimization of three factors—gradient time (t_G), temperature (T) and pH—to refine the separation conditions of amlodipine and its seven impurities, described in the European Pharmacopoeia (EP) across eight different L1-type Ultra-High Performance Liquid Chromatography (UHPLC) columns. Initially, a single linear gradient method provided baseline resolution on only one column. However, by using 3-D models as a feasibility tool to explore all possible separation conditions, it was demonstrated, that all columns could achieve baseline separation, albeit with varying degrees of robustness [40]. A similar modeling strategy was applied to another combination drug (amlodipine and bisoprolol) and its EP-specified impurities across 24 out of 25 state-of-the-art UHPLC stationary phases [41]. Later, in collaboration with Rácz, a 3-D modeling study was published to visualize column MODRs and reveal batch-to-batch variations in commercial bridged ethylene-hybrid (BEH) narrow-bore columns [42]. Another notable application from this team involved advanced 3-D experimental model designs, including an 18-run model developed to simultaneously apixaban synthesis route [43,44]. Following similar design schemes, comprehensive t_G-T-pH models aided the update of albendazole’s old EP method [45]. Apart from RP-cases, simple 2-D t_G-pH separation models were successfully employed in cation-exchange chromatography (CAX) for the separation of digested monoclonal antibody (mAb) charge variants [46]. These examples highlight the versatility and practical value of chromatography-based modeling approaches in pH modeling-, and optimization.

In our earlier study, we also introduced a successful DS modeling methodology to substantiate both the selectivity differences and similarities among various USP L1-type stationary phases. The results revealed an intricate dynamism between key system components, highlighting the complex, multidimensional relationships involving the stationary phase, applied method conditions and specific sample analytes. In this example we found DS-modeling particularly valuable for characterizing each separation system as a unique fingerprint, allowing for more effective comparisons. This chromatographic “in vivo” methodology proved to be extremely sensitive, offering much deeper insights, than traditional simple column characterization-, and comparison-methods [47,48].

Building on this methodical approach, we revisited the topic of eluent pH—a crucial factor in separation results, that has been discussed in only a limited number of technical reviews. To demonstrate the practical utility of this approach, we selected terazosin, an active pharmaceutical ingredient, along with a few impurities, exhibiting both basic and neutral characteristics. These substances, along with their EP-specified impurities, had been thoroughly investigated in previous works, resulting in the development of an LC-MS and LC-UV impurity profiling method. The latter was adopted by the EP and published in Pharm Europa, issue 32.2 [49].

With this background, the primary aim of our current research was to address a common challenge in everyday laboratory practice: Understanding the impact of pH, when using volatile versus non-volatile buffer systems. To achieve this, we once again utilized established 3-D (t_G-T-pH) DS-models of the DryLab modeling tool, combined with other advanced features of the software such as Design Space Comparison (DSC) and Multi-Attribute Modeling (MAM), available in the latest software installation.

2. Materials and methods/experimental part

2.1. Chemicals

Throughout the analyses, the aqueous mobile phase (eluent A) consisted of either a 10 mM phosphate or 10 mM acetate buffer, freshly prepared from the corresponding acid (orthophosphoric acid or acetic acid) and base (sodium, ammonium, potassium or lithium hydroxide). Avoiding the work with crystalline salts ensured better control over buffer molarity. For dilution, ultrapure water was obtained using an ELGA Purelab UHQ system (ELGA, Lane End, UK). The organic mobile phase (eluent B) was acetonitrile (ACN) (Merck, Darmstadt, Germany). Reference standards—terazosin and impurities A, B, D, and E—were sourced from the European Directorate for the Quality of Medicines & HealthCare (EDQM). The sample solvent consisted of methanol/water (70:30, V:V).

2.2. Equipment, software

DS modeling experiments were conducted on a Waters Acquity™ Classic UPLC system equipped with a binary solvent delivery pump, an autosampler, and a photodiode array detector. The chromatographic system had a 5 μL injection loop and a 500 nL flow cell, with a system dwell volume (V_D) measured as 100 μL. Instrument control and data acquisition were managed using Empower CDS (Waters, Milford, USA), with chromatographic processing performed at 248 nm.

DS models were developed using DryLab (version 4.6) HPLC-modeling software (Molnár-Institute, Berlin, Germany). pH adjustments were performed using an MP 225 pH-meter (Mettler-Toledo, Greifensee, Switzerland). Buffer capacity calculations and plotting were programmed in Python using Anaconda 3 (Anaconda Inc.), an open-source software package.

2.3. Stationary phase and buffer selection

To evaluate pH-dependent selectivity using different buffers, we selected two standard C18 stationary phases: Acquity™ HSS C18 and HSS C18 SB, both in narrow-bore formats (50 × 2.1 mm). Due to their distinct surface coverage—high for HSS C18 and low for HSS C18 SB—these phases expected to provide reasonably different selectivity contributions, particularly under the chosen experimental conditions.

Regarding buffer selection, our primary goal was to assess the practical feasibility of replacing a non-volatile buffer (sodium phosphate) with a volatile alternative (ammonium acetate) while maintaining identical pH ranges. To reduce the added experimental complexity, we fixed the buffer concentration at 10 mM, which is within the commonly used range (5–10 mM) for these small column formats [10].

3. Theory and calculations

3.1. Calculated buffer capacities

Buffer capacity (β) is a quantitative measure of the resistance of a buffer solution to pH change on addition of acid and/or base. It can be represented as the amount of strong acid or base necessary to the change pH with an infinitesimal unit.

$$\beta = \frac{dc_b}{dpH} = -\frac{dc_a}{dpH} \tag{1}$$

where c_a and c_b is the concentration of the strong acid and base, respectively. For weak monovalent acids or bases, the following general formula can be used for the calculation of buffer capacity.

$$\beta = \ln 10\left([H^+] + \frac{k_w}{[H^+]} + c_{tot}\frac{[H^+]\ K_a}{(K_a\ +\ [H^+])^2}\right) \tag{2}$$

where c_{tot} is the total concentration of the weak acid or base used as buffer, K_a its dissociation constant, and k_w the ionic product of water ($k_w = 10^{-14}$).

When more different types of monovalent weak acids and/or bases present in the solution, the third term in the parenthesis should be written for all buffer compounds.

$$\beta = \ln 10\left([H^+] + \frac{k_w}{[H^+]} + \sum_{i=1}^{n} c_{tot,i}\frac{[H^+]\ K_{a,i}}{(K_{a,i}\ +\ [H^+])^2}\right) \tag{3}$$

These simple equations stand true for a monovalent weak acids or bases. However, in case of multivalent acids such as the trivalent phosphoric acid, each of the dissociation steps ($K_{a,1}$, $K_{a,2}$, $K_{a,3}$) should be considered. In this case Eq. (2) changes to a much more complex expression:

$$\beta = \ln 10\left([H^+] + \frac{k_w}{[H^+]} + c_{tot}[H^+]\frac{p - q\rho}{\rho^2}\right) \tag{4}$$

where

$$p = \left(3\kappa_3 + 2\kappa_2[H^+] + \kappa_1[H^+]^2\right)\left(\kappa_2 + 2\kappa_1[H^+] + 3[H^+]^2\right) \tag{5}$$

$$q = 2(\kappa_2 + \kappa_1[H^+]) \tag{6}$$

$$\rho = K_{a,3}\ K_{a,2}\ K_{a,1}\ + K_{a,2}\ K_{a,1}\ [H^+] + K_{a,1}\ [H^+]^2 + [H^+]^3 \tag{7}$$

$$\rho = \kappa_3 + \kappa_2[H^+] + \kappa_1[H^+]^2 + [H^+]^3 \tag{8}$$

and κ_i is the product of the first i dissociation constants (i.e. $\kappa_2 = K_{a,2}\ K_{a,1}$). It should be noted, however, that the buffer capacity of most multivalent acids and bases can be precisely estimated using Eq. (3), as if each differently dissociated species were an independent buffer compound.

The calculated β-values plotted as dependence of pH is presented in Fig. 1 for phosphate, and ammonium acetate buffers.

3.2. Terazosin impurity analysis—Research history

The separation of terazosin from its European Pharmacopeia-specified impurities has been successfully addressed in two research studies. In the first study, the separation of 10 related impurities (Imp A, B, C, E, J, K, L, M, N and O) was achieved within approximately 5 min. This method, designed for use with a mass spectrometer, required a volatile buffer or additive. The use of 0.1 % NH_4OH (pH = 10.7) proved ideal, offering reasonable retention for the poorly retained Imp N and L, maintaining stability for the pH-sensitive Imp N and avoiding additive solubility issues. Additionally, a systematic design space modeling approach identified optimal conditions for gradient settings (t_G), temperature (T) and ternary composition (t_C, %MeOH in AcN). However, a key limitation of this method was its reliance on an MS setup, which is not always accessible in QC laboratories. Furthermore, the use of a bridged-ethylene-type (BEH) stationary phase (Acquity™ CSH C18), capable of withstanding alkaline conditions, restricted its broader applicability on other conventional silica-based columns [50].

In subsequent research, a more general method was developed utilizing a simple LC-UV setup with a perfluorinated stationary phase under slightly acidic, pH-control conditions (0.1 % perchloric acid). This approach not only separated the 10 specified impurities but was also capable of resolving five other “rare” impurities (Imp D, H, G, F and I). Moreover, leveraging recent design DSC tools, equivalent setpoints for competitive pentafluoro-phases were identified, accommodating two batches of both the primary and replacement columns (Fig. 2).

3.3. Design space modeling and comparison

Building on the established history of terazosin impurity analysis, the goal of this study was not to develop a novel method but rather to leverage our prior experience with these molecules in a proof-of-concept study. To this end, we deliberately selected alkaline conditions, under which the basic molecules (terazosin, Imp A, Imp D and Imp E) would undergo ionic changes, while the neutral impurity (Imp B) was expected to remain unaffected.

Once the model substances were selected, we established a modeling workflow consisting of three consecutive steps, as shown in Fig 3. Following the initial selection of two stationary phases, the modeling framework was structured with consideration of appropriate modeling input ranges, as previously reported in other studies [45,48,51]. The experimental setup included two linear gradient experiments with gradient times of 3 and 9 min (t_{G1} and t_{G2}) and fixed start- and end- %B values (20–50 %B). Additionally, two temperatures (T_1 = 20 °C and T_2 = 50 °C) and a relatively broad pH range (6.0–8.0) were selected for covering the whole pH range of the selected buffers, including five experimental steps (pH_1–pH_5) with pH increments of no >0.5 unit each. Overall, this DoE framework resulted in 2 × 2 × 5 = 20 input runs per modeled separation system, totaling 80 runs, that in exchange, allowed us to comprehensively track separation changes between the two buffer systems and the two stationary phases. The experiments were conducted in a run order as described by Rácz [42], ensuring proper equilibration and optimizing overall runtime efficiency—completing the full set of model input experiments in approximately 3 × 4 = 12 h. Finally, the results were processed and imported into the software platform for peak

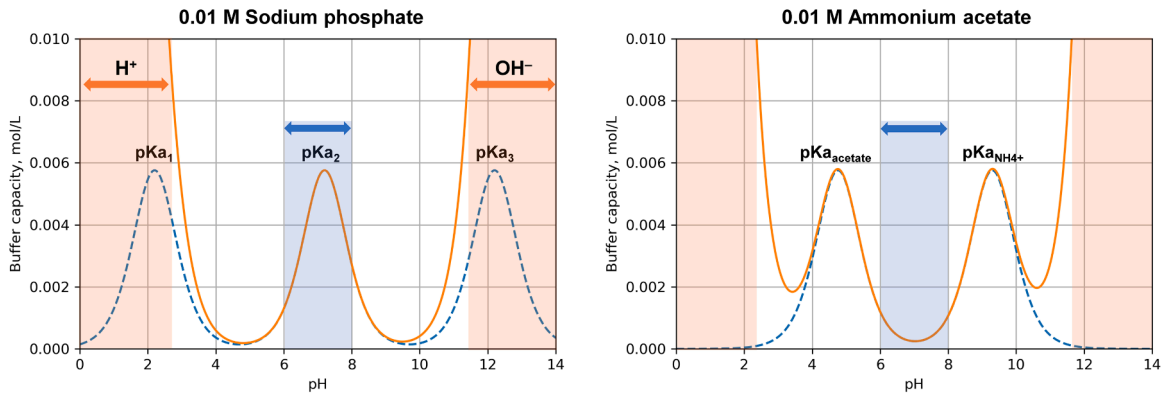


Fig. 1. Calculated buffer capacities (or indexes) of the two studied 0.01 M buffer systems. As seen, buffering capacities across the 0–14 pH-range are small especially, when compared to strong acid (H_3O^+/H_2O) or base (OH^-/H_2O). In the selected pH-range (6.0–8.0) phosphate can give some, whereas ammonium acetate practically no buffering capacity at all.

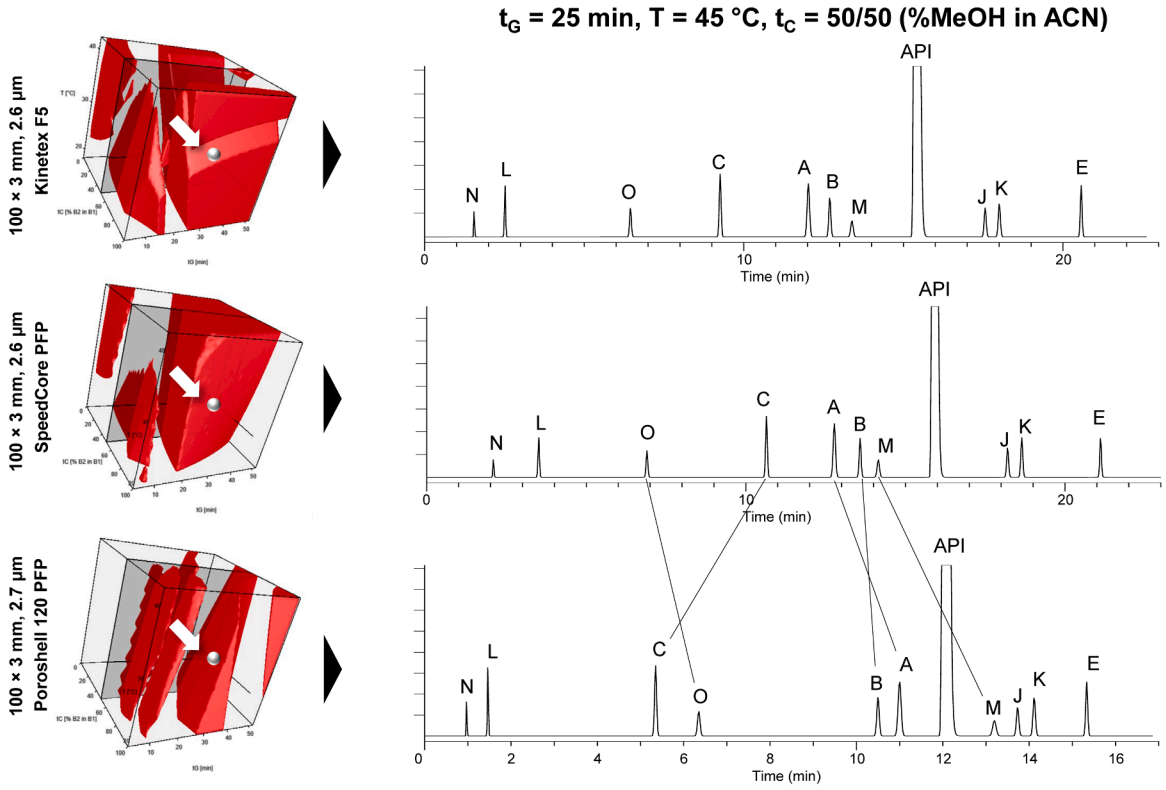


Fig. 2. Separation changes of terazosin and 10 European Pharmacopeia (EP) specified impurities, shown by the acquired MODRs on three competitive PFP-type stationary phases. These models originate from [49] and were used to update the old EP compendial methods. Here, at the same, selected working point (t_G = 25 min, T = 45 °C and t_C = 50 %MeOH in ACN) the Kinetex F5 and Speedcore F5 columns are considered conveniently interchangeable. However, Poroshell 120 PFP shows very different selectivity profile, resulting in several peak elution alterations.

tracking and in-depth model analysis.

4. Results and discussion

4.1. General considerations in choosing suitable pH-conditions

While pH is often considered a key parameter in chromatographic separation, its actual effect on retention is highly dependent on the nature of the analytes and the buffer system used. It should be noted, that in several cases, pH has no significant effect on peak retention. For instance, neutral compounds, such as impurity B in our modeling sample, lacks ionizable functional groups, leading to consistent retention. Additionally, even ionizable compounds under pH-controlled conditions tend to maintain stable retention properties, which can be extremely beneficial in enhancing overall method robustness. Conversely, since H_3O^+ and OH^- exhibit strong buffering capacity, no significant differences are expected between identical pH values at either end of the pH range, regardless of the acidic or basic modifier used.

However, when the eluent pH falls within approximately $pK_a \pm 2$, it strongly influences the ionic state of analytes, thereby affecting their retention properties. As most analytes exhibit weak acidic or basic characteristics—like terazosin, Imp A, B and D—the intermediate pH range becomes particularly valuable for fine-tuning their selectivity. In this context, it is important to highlight that there are only a limited number of buffer systems suitable for use in the intermediate pH range, each differing in their effective pH range and buffering capacity, as

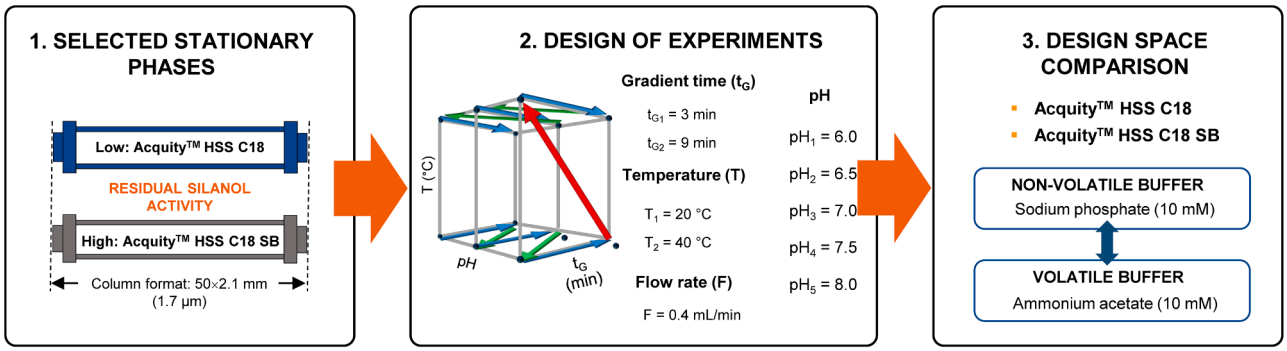


Fig. 3. Applied systematic development scheme for building up and comparing individual Design Space Models of the selected buffer systems on the two stationary phases.

illustrated in Fig. 1.

In the pursuit of selecting an appropriate pH—whether for maintaining pH control or optimizing selectivity—molecule-structure-based tools, that estimate log P and log d-pH relationships using specific descriptors can be considered. However, based on our previous experience, these predictive tools often yield inconsistent results across different software packages and fail to account for critical factors, such as applied method conditions and the physicochemical properties of specific columns. As a result, their utility is largely limited to preliminary knowledge acquisition rather than practical method optimization. For this reason, we relied exclusively on experimental measurements, rather than this type of predictive modeling.

4.2. *Acetate and phosphate buffers in pH-range of 6.0–8.0*

Indeed, our t_G-T-pH model results revealed unexpected developments in separation dynamics when analyzing the full modeling maps. To provide a clearer overview, Fig 4 displays only the baseline-separating MODR-areas alongside the observed elution order. These plotted regions exhibited distinct irregularities, with some showing strong similarities between buffer types, while others displayed significant differences. For instance, the comparative MODRs at low pH conditions (~pH 6.0–6.5) were nearly identical between phosphate and acetate buffers on both columns, indicating that convenient interchangeability of selectivity can be achieved in this range. Interestingly, the HSS C18 D→B→A→API and the HSS C18 SB A→B→D→API MODRs between the two buffers exhibited similar development characteristics, this similarity abruptly discontinued at around pH = 7.0 and progressed further following distinct trajectories. Consequently, when comparing MODRs of the two buffers under slightly alkaline conditions, they cannot be considered equivalent.

Furthermore, an analysis of the full MODR bodies for the two stationary phases revealed that there is no shared, intercolumn MODR that could provide both baseline resolution and an identical elution order.

A more detailed analysis of pH effects on chromatographic selectivity was conducted by examining chromatograms at a fixed gradient time and temperature. Fig. 5 and 6 display chromatograms recorded at 1 pH unit increments, allowing for the observation of subtle peak movements.

Contrary to typical trends, some unexpected retention shifts were observed, even on the well-covered HSS C18 column. While the basic compounds terazosin and impurity D exhibited the expected increase in retention with rising pH, impurity A did not follow this behavior.

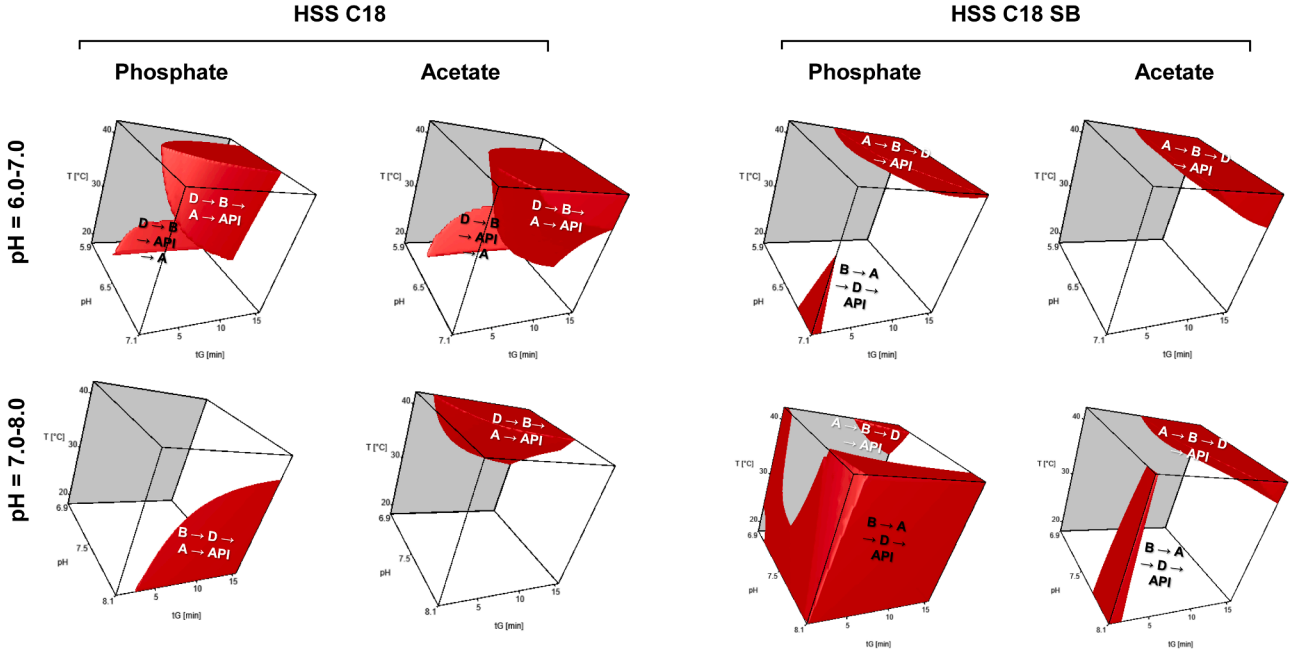


Fig. 4. Comparison of the red-displayed ($R_{s,crit.} \geq 1.5$) MODR areas of the two buffer systems on the selected stationary phases. The complete pH-range was bisected into two pH-models with pH = 7.0 being one end-value for both. Thus, the lower MODRs (7.0–8.0) can be considered as the respective continuation of the upper t_G-T-pH models.

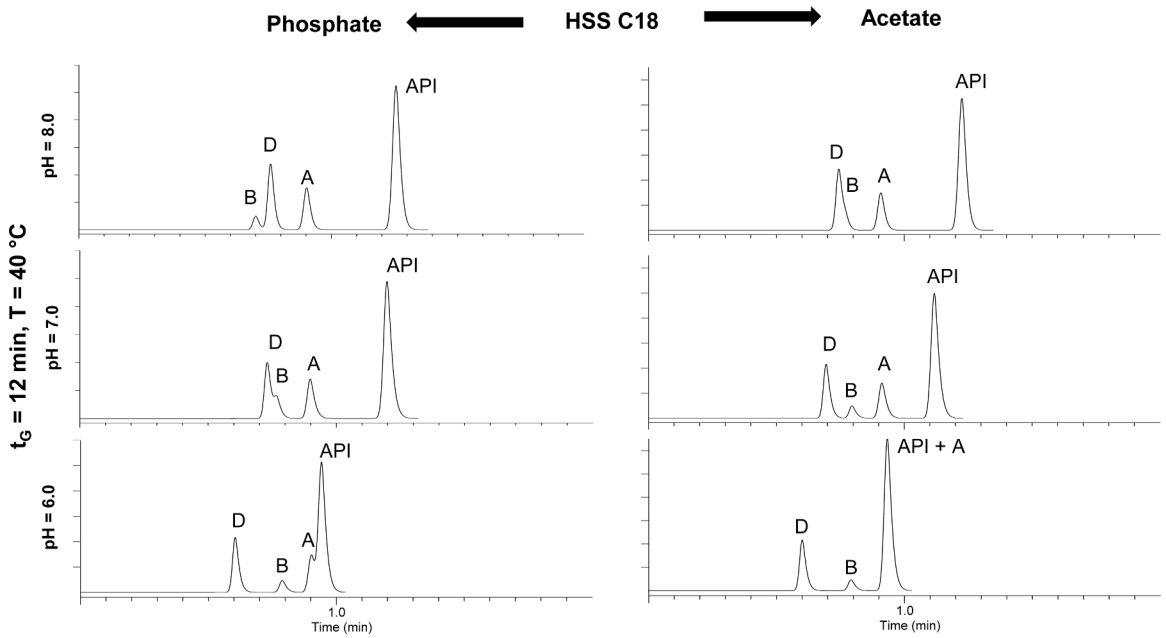


Fig. 5. Comparison of selected chromatograms at fixed gradient time (12 min), temperature (40 °C) and three selected pH-settings (6.0, 7.0 and 8.0) using the HSS C18 stationary phase which is a well-covered stationary phase with low residual silanol activity.

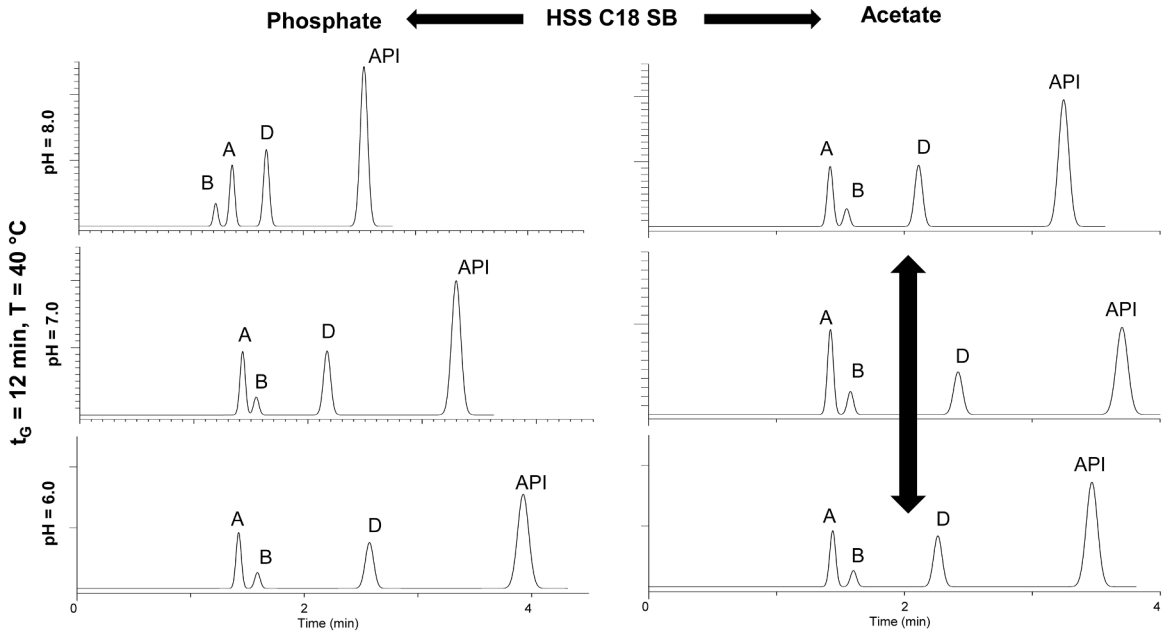


Fig. 6. Comparison of selected chromatograms at fixed gradient time (12 min), temperature (40 °C) and three selected pH-settings (6.0, 7.0 and 8.0) using the HSS C18 SB stationary phase which features a high residual silanol activity. Interestingly, the observed selectivities for acetate's pH=6.0 and 8.0 results are nearly identical.

Additionally, the neutral impurity B displayed a loss in retention, particularly under phosphate buffer conditions at pH 8.0.

Without drawing premature conclusions, one possible explanation for this behavior is the superimposed effect of pH, influenced by buffering capacity and the gradual activation of residual silanol groups, which are still present even on stationary phases with high surface coverage. Here, it can be estimated that the concentration of silanol groups before surface modification is about 8 μmol/m^2, which, given the surface coverage specifications of the HSS C18 column (3.2 μmol/m^2), suggests that approximately every second residual silanol site may be unreacted and contribute to either polar or electrostatic interactions, depending on the pH [52].

These effects were even more pronounced on the HSS C18 SB stationary phase (Fig. 6), which features a significantly lower surface coverage (~1.6 μmol/m^2). The presence of residual silanol groups is evident in the overall stronger retention observed under identical conditions for this column. However, the most intriguing finding was that retention trends followed an entirely different pattern, suggesting a whole different interplay between pH, surface interactions and the resulting selectivity on this phase.

Clearly, despite the same nominal pHs between the buffer systems, the chromatographic selectivity drastically changed when moving from

neutral to basic range. This phenomenon culminated in a single peak-order reversal at pH = 8.0, showing that these buffers are practically non-equivalent under the selected condition.

Another noteworthy observation was the retention shift of basic compounds. In phosphate buffer, all basic impurities exhibited a gradual loss in retention as pH increased. However, in acetate buffer, an unusual curved trend was observed: retention initially increased at pH 7.0, followed by a reversal at pH 8.0, returning almost to the original selectivity seen at pH 6.0. Meanwhile, impurity B remained anchored and impurity A showed a slight loss in retention. This suggests that for this particular analysis, interchangeable selectivities can be achieved for all pH-sensitive compounds at two distinct pH levels, offering a surprising flexibility in method development.

Finally, to validate our models, we arbitrarily selected two verification points (Fig. 7) for the more complex HSS C18 SB phase under slightly alkaline conditions (pH = 7.8). This pH region was intentionally chosen because the model predicted significant selectivity changes, particularly when comparing the two buffer systems.

At **Verification experiment 1** ($t_G = 6$ min, $T = 25$ °C), the phosphate buffer was expected to provide baseline separation, as indicated by the Critical Resolution Map (CRM). However, in the reality, broadened peak shapes prevented this from fully accomplishing. These at baseline broadened, non-Gaussian peaks suggest the presence of detrimental long-range ionic interactions, which can negatively impact peak-widths and thus, resolution of closely eluting compounds.

For the acetate buffer, the model predicted coelution, which was also experimentally confirmed. However, slight retention time shifts were observed for the basic impurity D and terazosin between the model and the verification experiment. This discrepancy may be attributed to minor pH adjustment errors when preparing the new buffer or the consequence of general instability of the acetate buffer due to its limited buffering capacity at this pH.

At **Verification experiment 2** ($t_G = 12$ min, $T = 35$ °C), an incomplete elution order change was observed, underscoring the risks of unintentionally substituting phosphate with acetate buffer. Similar to phosphate at **Verification experiment 1**, the baseline-separating area for acetate failed to achieve the critical resolution threshold ($R_{s,crit.} \geq 1.5$), as indicated by the initial modeling results.

In summary, while the modeling study provided valuable correlative knowledge, there is another crucial consideration in method design—although pH is a powerful tool for optimizing selectivity, the activated ionic sites can also negatively impact peak shapes. These effects may be mitigated by increasing buffer concentration or incorporating organic amines, if reasonable. However, given that the studied pH (~8.0) approaches the maximum operational limit for traditional silica-based stationary phases, potential pH-induced shifts (plus or minus) should be considered. As previously referenced in Claassens' research [12], method developers must consider additional factors such as expected column lifetime. If necessary, they should opt for stabilized, pH-resistant base materials—such as a BEH phase—or select a more suitable acidic

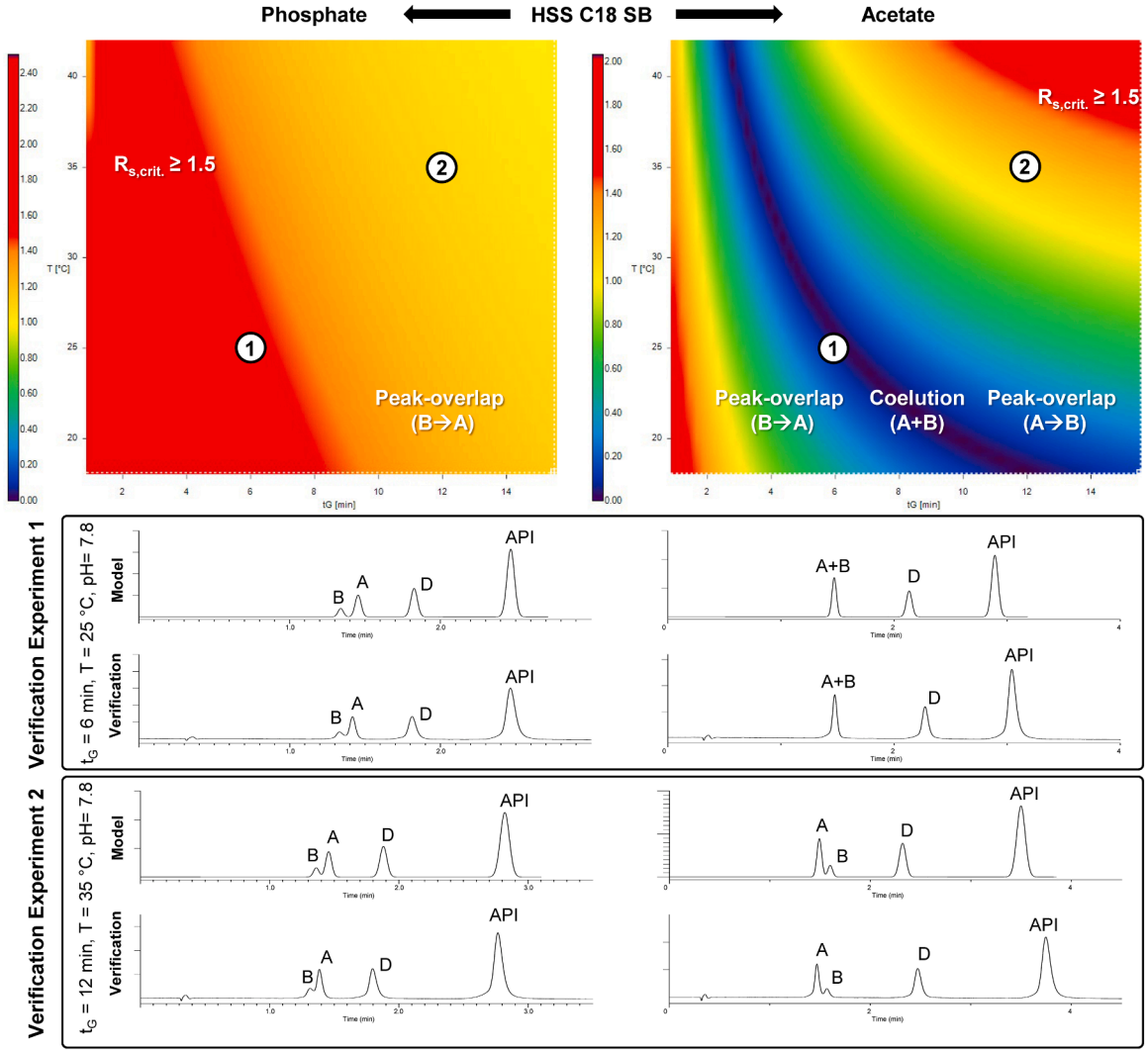


Fig. 7. Selected verification experiments (1 and 2) in the HSS C18 SB critical resolution map and corresponding model–experimental comparisons.

pH condition, as demonstrated in the referenced precursor studies.

4.3. "Salting-out" studies with NH_4^+, K^+, Na^+, Li^+ buffer cations

To further expand the scope of this research, we also explored whether, under the "sensitized", slightly basic pH conditions, replacing buffer cations could influence separation outcomes. For this purpose, we selected the residual silanol-rich HSS C18 SB phase and conducted an additional set of experiments under the previously outlined **Verification experiments 1 and 2**, using the same two buffers but with different cation types. The resulting chromatograms revealed some considerable changes in both selectivity and peak shapes.

Although Fig. 8 presents chromatograms arranged according to their hypothetical increasing Hofmeister series, the observed results did not fully follow the expected trend of increasing overall retention toward the most kosmotropic ammonium cation. Additionally, the basic peaks displayed an unusual curved retention development for the phosphate buffer, whereas a less pronounced, inconsistent retention for the acetate buffer. In some cases, this was accompanied by poor peak shapes (e.g., lithium acetate in **Supplementary Fig. 1**), though these significantly improved at elevated temperatures.

This aligns with the understanding that surface energetics of colloidal structures can shift rapidly with changes in pH and salt concentration, potentially leading to an altered or even reversed Hofmeister-effects [53]. A similar phenomenon may also occur on a molecular level between the stationary phase, mobile phase and sample, particularly in the absence of acetate's strong pH-dampening effects. This could explain the heterogeneous retention behavior and deteriorated peak shapes observed in our study.

Interestingly, the selectivity difference between identical cations and their respective phosphate–acetate anions appeared less critical than by moving from one cation to the next. For instance, simply replacing volatile ammonium salts with non-volatile Li^+, K^+, or Na^+ in both buffers led to a rapid elution order alteration for the Imp A and B pair, substantiating an added influence of cation selection.

Ultimately, these findings emphasize the necessity of custom-built DS models, which yield quantitative knowledge of all separation outcomes within the studied separation system. As a result, they offer much-needed support in elucidating basic chromatographic results instead of delving into overly complex synergistic and antagonistic influences, thereby facilitating practical method development.

5. Conclusion

In reversed-phase chromatography (RPC), defining pH and reliably accounting for its effects on chromatographic retention is inherently complex. Numerous factors influence retention, including mobile-phase properties (organic modifier amount and composition, temperature, buffer type), stationary phase characteristics (hydrophobicity, polar and ionic properties), specific analyte properties. However, these factors are all tightly connected and together shape a pH-dependent retention behavior as well. As a result, tangible pH effects in RPC cannot be reliably assessed without an extensive and systematic modeling support.

Bearing this in mind, our study addressed a common challenge by comparing the interchangeability of volatile acetate and non-volatile phosphate buffers. To achieve this, we selected two stationary phases with differing residual silanol activity (HSS C18 and HSS C18 SB) and a very simple modeling sample (terazosin) containing a few basic and one neutral impurity. We utilized established 3D (t_G-T-pH) models with the DryLab modeling tool to conduct an in-depth analysis of separation behavior in relation to buffer type and pH (range 6.0–8.0).

The modeled resolution spaces (MODRs) revealed that acetate and phosphate buffers can, under certain conditions, be interchanged. However, in other cases, they exhibited very distinct selectivities, making them non-alternatives, primarily depending on the pH and also other applied conditions. This underscores the multidimensional nature of chromatographic separations and suggests the need for powerful modeling tools to obtain reliable pH-effect assessments. These findings are also supported by the latest Analytical Quality by Design (AQbD) regulatory guidelines, which advocate the use of systematic modeling approaches in method development.

As a final research outlook, we also conducted an exploratory set of experiments to investigate potential "salting-out" effects when using different NH_4^+, K^+, $Na^+$and Li^+ buffer cations. The results under the tested conditions revealed some unexpected selectivity shifts, highlighting the need for caution when substituting buffer cations without careful consideration.

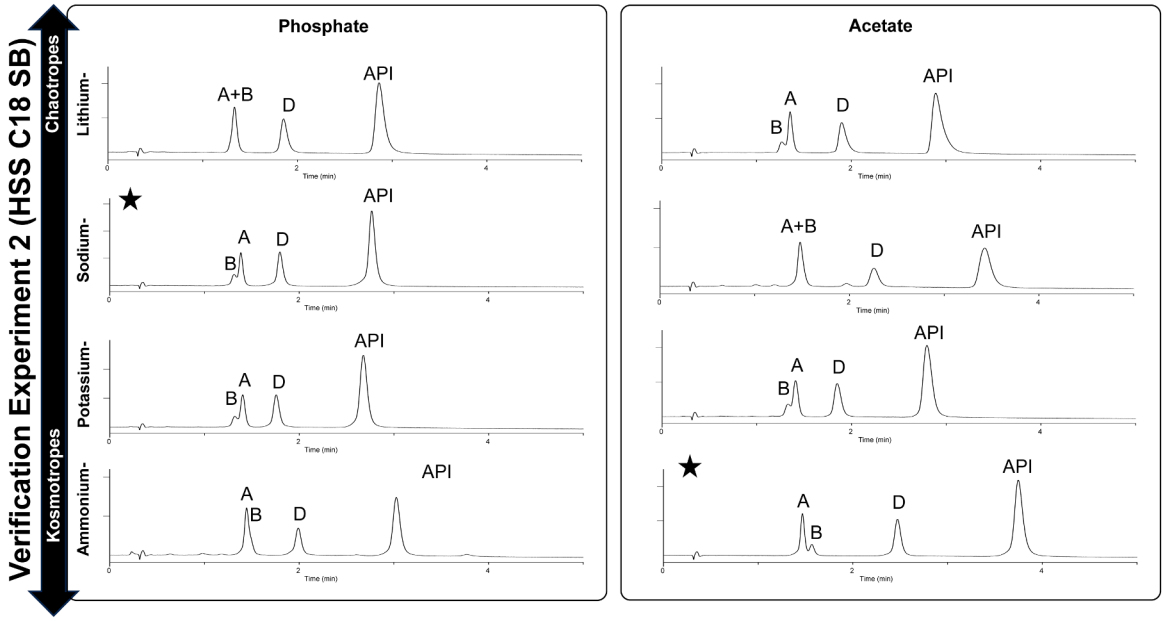


Fig. 8. Salt effects studied under "Verification Experiment 2″ conditions (t_G = 12 min, T = 35 °C, pH = 7.8), comparing four buffer cations arranged in order of increasing kosmotropic properties according to the Hofmeister series (NH_4^+>K^+>Na^+>Li^+) The two marked chromatograms represent the initially tested volatile and non-volatile buffer systems, demonstrating that they are not interchangeable in this case.

CRediT authorship contribution statement

Arnold Zöldhegyi: Writing – original draft, Methodology, Investigation. **Barnabás Soós:** Methodology, Investigation. **Krisztián Horváth:** Writing – review & editing. **Imre Molnár:** Writing – review & editing. **Róbert Kormány:** Writing – original draft, Methodology, Investigation, Conceptualization.

Declaration of competing interest

The authors declare that they have no known competing financial interests or personal relationships that could have appeared to influence the work reported in this paper.

Acknowledgement

The authors would like to thank Markus Molnár, Hans-Jürgen Rieger (Molnár-Institute for Applied Chromatography, Berlin, Germany) and Botond Bogáti (Gedeon Richter Plc Hungary) for their helpful advice and comments.

Supplementary materials

Supplementary material associated with this article can be found, in the online version, at doi:10.1016/j.chroma.2025.465951.

Data availability

Data will be made available on request.

References

[1] J.W. Dolan, L.R. Snyder, Chapter 13 - method development in liquid chromatography. Liquid Chromatography Fundamentals and Instrumentation (Third Edition), Elsevier, 2023, pp. 323–336, https://doi.org/10.1016/B978-0-323-99968-7.00032-1.
[2] I. Molnár, Searching for robust HPLC methods: csaba Horváth and the Solvophobic theory, Chromatographia 62 (2005) 7–17, https://doi.org/10.1365/s10337-005-0645-1.
[3] Cs. Horváth, W. Melander, I. Molnár, Solvophobic interactions in liquid chromatography with nonpolar stationary phases – solvophobic interactions part I, J. Chromatogr. 125 (1976) 129–156, https://doi.org/10.1016/S0021-9673(00)93816-0.
[4] Cs. Horváth, W. Melander, I. Molnár, Liquid chromatography of ionogenic substances with nonpolar stationary phases – solvophobic interactions part II, Anal. Chem. 49 (1977) 142–154, https://doi.org/10.1021/ac50009a044.
[5] Cs. Horváth, W. Melander, I. Molnár, P. Molnár, Enhancement of retention by ion-pair formation in liquid chromatography with nonpolar stationary phases – solvophobic interactions part III, Anal. Chem. 49 (1977) 2295–2305, https://doi.org/10.1021/ac50022a048.
[6] S. Moldoveanu, V. David, Chapter 7 - mobile phases and their properties. Essentials in Modern HPLC Separations, Elsevier, 2022, pp. 207–269, https://doi.org/10.1016/B978-0-323-91177-1.15002-1.
[7] G.W. TIndall, Mobile-phase buffers, part I: the interpretation of pH in partially aqueous Mobile phases, LC. GC. N. Am. 20 (11) (2002) 1028–1032.
[8] M. Rosés, Determination of the pH of binary mobile phases for reversed-phase liquid chromatography, J. Chrom. A 1037 (2004) 289–294, https://doi.org/10.1016/j.chroma.2003.12.063.
[9] G.W. Tindall, Mobile-phase buffers, part II: buffer selection and capacity, LC. GC. N. Am. 20 (12) (2002) 1114–1118.
[10] J.W. Dolan, "A guide to HPLC and LC-MS buffer selection". https://www.hplc.eu/Downloads/ACE_Guide_BufferSelection.pdf.
[11] M.C. García-Alvarez-Coque, J.R. Torres-Lapasió, M.J. Ruiz-Angel, J.A. Navarro-Huerta, Chapter 7 - secondary chemical equilibria in reversed-phase liquid chromatography. Liquid Chromatography Fundamentals and Instrumentation (Third Edition), Elsevier, 2023, pp. 121–144, https://doi.org/10.1016/B978-0-323-99968-7.00012-6.
[12] H.A. Claessens, M.A. Straten, J.J. Kirkland, Effect of buffers on silica-based column stability in reversed-phase high-performance liquid chromatography, J. Chrom. A 728 (1–2) (1996) 259–270, https://doi.org/10.1016/0021-9673(95)00904-3.
[13] G.W. Tindall, R.L. Perry, Explanation for the enhanced dissolution of silica column packing in high pH phosphate and carbonate buffers, J. Chrom. A 988 (2) (2002) 309–312, https://doi.org/10.1016/S0021-9673(02)02085-X.
[14] X. Subirats, E. Bosch, M. Rosés, Buffer considerations for LC and LC-MS, LC. GC. N. Am. 27 (11) (2009) 1000–1004.
[15] G.W. Tindall, Mobile phase buffers, part III: preparation of buffers, LC. GC. N. Am. 21 (1) (2003) 28–32.
[16] D.R. Stoll, D.M. Makey, Mobile phase buffers in LC: effect of buffer preparation method on retention repeatability, LC. GC. N. Am. 37 (7) (2019) 444–449.
[17] A.P. Schellinger, P.W. Carr, Solubility of buffers in acqueous-organic eluents for reversed-phase chromatography, LC. GC. N. Am. 22 (6) (2004) 544–548.
[18] J. Barbosa, V. Sanz-Nebot, Autoprotolysis constants and standardization of the glass electrode in acetonitrile-water mixtures. Effect of solvent composition, Anal. Chim. Acta 244 (1991) 183–191, https://doi.org/10.1016/s0003-2670(00)82496-4.
[19] J.W. Dolan, Back to basics: the role of pH in retention and selectivity, LC. GC. N. Am. 35 (1) (2017) 22–28.
[20] International Concil for Harmonisation of Technical Requirements for Pharmaceuticals for Human Use, "Technical and regulatory considerations for pharmaceutical lifecycle management Q12" 20 November 2019. https://database.ich.org/sites/default/files/Q12_Guideline_Step4_2019_1119.pdf.
[21] International Concil for Harmonisation of Technical Requirements for Pharmaceuticals for Human Use, "Analytical procedure development Q14" 1 November 2023. https://database.ich.org/sites/default/files/ICH_Q14_Guideline_2023_1116_1.pdf.
[22] International Concil for Harmonisation of Technical Requirements for Pharmaceuticals for Human Use, "Validation of analytical procedures Q2(R2)" 1 November 2023. https://database.ich.org/sites/default/files/ICH_Q2%28R2%29_Guideline_2023_1130.pdf.
[23] R.J. Laub, J.H. Purnell, Criteria for the use of mixed solvents in gas—Liquid chromatography, J. Chrom. A 112 (1975) 71–79, https://doi.org/10.1016/S0021-9673(00)99943-6.
[24] S.N. Deming, M.L.H. Turoff, Optimization of reverse-phase liquid chromatographic separation of weak organic acids, Anal. Chem. 50 (4) (1978) 546–548, https://doi.org/10.1021/ac50026a003.
[25] W.P. Price, R. Edens, D.L. Hendrix, S.N. Deming, Optimized reverse-phase high-performance liquid chromatographic separation of cinnamic acids and related compounds, Anal. Biochem. 93 (1978) 233–237, https://doi.org/10.1016/S0003-2697(79)80143-8.
[26] B. Sachok, R.C. Kong, S.N. Deming, Multifactor optimization of reversed-phase liquid chroamtographic separations, J. Chrom. A 199 (1980), https://doi.org/10.1016/S0021-9673(01)91383-4, 327-325.
[27] J.W. Dolan, D.C. Lommen, L.R. Snyder, High-performance liquid chromatographic computer simulation based on a restricted multi-parameter approach—I. Theory and verification, J. Chrom. A 535 (1990) 55–74, https://doi.org/10.1016/S0021-9673(01)88935-4.
[28] L.R. Snyder, J.W. Dolan, D.C. Lommen, High-performance liquid chromatographic computer simulation based on a restricted multi-parameter approach—II. Application, J. Chrom. A 535 (1990) 75–92, https://doi.org/10.1016/S0021-9673(01)88936-6.
[29] J.A. Lewis, D.C. Lommen, W.D. Raddatz, J.W. Dolan, L.R. Snyder, I. Molnár, Computer simulation for the prediction of separation as a function of pH for reversed-phase high-performance liquid chromatography—I. Accuracy of a theory-based model, J. Chrom. A 592 (1–2) (1992) 183–195, https://doi.org/10.1016/0021-9673(92)85085-8.
[30] J.A. Lewis, J.W. Dolan, L.R. Snyder, I. Molnár, Computer simulation for the prediction of separation as a function of pH for reversed-phase high-performance liquid chromatography—II. Resolution as a function of simultanous change in pH and solvent strength, J. Chrom. A 592 (1–2) (1992) 197–208, https://doi.org/10.1016/0021-9673(92)85086-9.
[31] P.L. Zhu, L.R. Snyder, J.W. Dolan, N.M. Djordjevic, D.W. Hill, L.C. Sander, T. J. Waeghe, Combined use of temperature and solvent strength in reversed-phase gradient elution: I. Predicting separation as a function of temperature and gradient conditions, J. Chrom. A 756 (1–2) (1996) 21–39, https://doi.org/10.1016/S0021-9673(96)00721-2.
[32] P.L. Zhu, J.W. Dolan, L.R. Snyder, Combined use of temperature and solvent strength in reversed-phase gradient elution: II. Comparing selectivity for dIfferent samples and systems, J. Chrom. A 756 (1–2) (1996) 41–50, https://doi.org/10.1016/S0021-9673(96)00722-4.
[33] P.L. Zhu, J.W. Dolan, L.R. Snyder, D.W. Hill, L. Van Heukelem, T.J. Waeghe, Combined use of temperature and solvent strength in reversed-phase gradient elution: III. Selectivity for ionizable samples as a function of sample type and pH, J. Chrom. A 756 (1–2) (1996) 51–62, https://doi.org/10.1016/S0021-9673(96)00723-6.
[34] P.L. Zhu, J.W. Dolan, L.R. Snyder, N.M. Djordjevic, D.W. Hill, J.-T. Lin, L.C. Sander, L. Van Heukelem, Combined use of temperature and solvent strength in reversed-phase gradient elution: IV. Selectivity for neutral (non-ionized) samples as a function of sample type and other separation conditions, J. Chrom. A 756 (1–2) (1996) 63–72, https://doi.org/10.1016/S0021-9673(96)00724-8.
[35] J.W. Dolan, L.R. Snyder, N.M. Djordjevic, D.W. Hill, D.L. Saunders, L. Van Heukelem, T. Waeghe, Simultaneous variation of temperature and gradient steepness for reversed-phase high-performance liquid chromatography method development: I. Application to 14 different samples using computer simulation, J. Chrom. A 803 (1–2) (1998) 1–31, https://doi.org/10.1016/S0021-9673(97)01293-4.
[36] J.W. Dolan, L.R. Snyder, D.L. Saunders, L. Van Heukelem, Simultaneous variation of temperature and gradient steepness for reversed-phase high-performance liquid chromatography method development: II. The use of further changes in conditions, J. Chrom. A 803 (1–2) (1998) 33–50, https://doi.org/10.1016/S0021-9673(97)01294-6.

[37] T.H. Jupille, J.W. Dolan, L.R. Snyder, I. Molnár, Two-dimensional optimization using DIfferent pairs of variables for the reversed-phase high-performance liquid chromatographic separation of a mixture of acidic compounds, J. Chrom. A 948 (1–2) (2002) 35–41, https://doi.org/10.1016/S0021-9673(01)01587-4.
[38] I. Molnár, H.-J. Rieger, K. Monks, Aspects of the "design space" in high pressure liquid chromatography method development, J. Chromatogr. A 1217 (19) (2010) 3193–3200, https://doi.org/10.1016/j.chroma.2010.02.001.
[39] I. Molnár, K. Monks, From Csaba Horváth to quality by Design: visualizing design space in selectivity exploration of HPLC separations, Chromatographia 73 (2011) 5–14, https://doi.org/10.1007/s10337-011-1968-8.
[40] R. Kormány, I. Molnár, H.-J. Rieger, Exploring better column selectivity choices in ultra-high performance liquid chromatography using Quality by Design principles, J. Pharm. Biomed. Anal. 80 (2013) 79–88, https://doi.org/10.1016/j.jpba.2013.02.028.
[41] R. Kormány, I. Molnár, J. Fekete, D. Guillarme, Sz. Fekete, Robust UHPLC separation method development for multi-API product amlodipine and bisoprolol: the impact of column selection, Chromatographia 77 (2014) 1119–1127, https://doi.org/10.1007/s10337-014-2633-9.
[42] N. Rácz, R. Kormány, J. Fekete, I. Molnár, Establishing column batch repeatability according to Quality by Design (QbD) principles using modeling software, J. Pharm. Biomed. Anal. 108 (2015) 1–10, https://doi.org/10.1016/j.jpba.2015.01.037.
[43] N. Rácz, R. Kormány, Retention modeling in an extended knowledge space, Chromatographia 81 (2018) 585–594, https://doi.org/10.1007/s10337-017-3466-0.
[44] R. Kormány, N. Rácz, Sz. Fekete, K. Horváth, Development of a fast and robust UHPLC method for Apixaban In-process control analysis, Molecules. 26 (12) (2021) 3505, https://doi.org/10.3390/molecules26123505.
[45] E. Ferencz, È.-K. Kelemen, M. Obreja, E. Sipos, S. Vida, M. Urkon, Z.-I. Szabó, Computer-assisted UHPLC method development and optimization for the determination of albendazole and its related substances, J. Pharm. Biom. Anal. 203 (2021) 114203, https://doi.org/10.1016/j.jpba.2021.114203.
[46] B. Duivelshof, A. Zöldhegyi, D. Guillarme, M. Lauber, Sz. Fekete, Expediting the chromatographic analysis of COVID-19 antibody therapeutics with ultra-short columns, retention modeling and automated method development, J. Pharm. Biomed. Anal. 221 (2022) 115039, https://doi.org/10.1016/j.jpba.2022.115039.
[47] R. Kormány, B. Soós, K. Horváth, Updating the European Pharmacopoeia impurity profiling method for cetirizine and suggesting alternative column, using design space comparison, J. Pharm. Biomed. Anal. 237 (2024) 115776, https://doi.org/10.1016/j.jpba.2023.115776.
[48] A. Zöldhegyi, K. Horváth, R. Kormány, Revisiting column selectivity choices in ultra-high performance liquid chromatography–Using multidimensional analytical design spaces to identify column equivalency, J. Chrom. A 1719 (2024) 464738, https://doi.org/10.1016/j.chroma.2024.464738.
[49] D. Enesei, I. Kapui, Sz. Fekete, R. Kormány, Updating the European Pharmacopoeia impurity profiling method for terazosin and suggesting alternative columns, J. Pharm. Biomed. Anal. 187 (2020) 113371, https://doi.org/10.1016/j.jpba.2020.113371.
[50] R. Kormány, I. Molnár, J. Fekete, Renewal of an old European Pharmacopoeia method for Terazosin using modeling with mass spectrometric peak tracking, J. Pharm. Biomed. Anal. 137 (2017) 8–15, https://doi.org/10.1016/j.jpba.2016.11.050.
[51] N. Rácz, I. Molnár, A. Zöldhegyi, H.-J. Rieger, R. Kormány, Simultaneous optimization of mobile phase composition and pH using retention modeling and experimental design, J. Pharm. Biomed. Anal. 160 (2018) 336–343, https://doi.org/10.1016/j.jpba.2018.07.054.
[52] U.D. Neue, Chapter 10 – Reversed-phase chromatography. HPLC Columns Theory Technology and Practice, Wiley-VCH, New York, 1997, pp. 183–216. ISBN: 978-0-471-19037-0.
[53] N. Schwierz, D. Horinek, U. Sivan, R.N. Netz, Reversed Hofmeister series—The rule rather than the exception, Curr. Opin. Colloid. Interface Sci. 23 (2016) 10–18, https://doi.org/10.1016/j.cocis.2016.04.003.